



Volume 106

2020

p-ISSN: 0209-3324

e-ISSN: 2450-1549

DOI: <https://doi.org/10.20858/sjsutst.2020.106.4>



Silesian  
University  
of Technology

Journal homepage: <http://sjsutst.polsl.pl>

---

**Article citation information:**

Jírová, R., Pešík, L. Identification and verification of dynamic parameters for the welding manipulator. *Scientific Journal of Silesian University of Technology. Series Transport*. 2020, **106**, 51-61. ISSN: 0209-3324. DOI: <https://doi.org/10.20858/sjsutst.2020.106.4>.

**Radka JÍROVÁ<sup>1</sup>, Lubomír PEŠÍK<sup>2</sup>**

**IDENTIFICATION AND VERIFICATION OF DYNAMIC PARAMETERS FOR THE WELDING MANIPULATOR**

**Summary.** Welding production lines are indispensable parts of the production processes in the automotive industry. In many cases, the production line operation is ensured by equipment with linear conveyors or robots, wherein linear guiding systems are basic elements of these manipulators. The failure of some linear guiding system may lead to significant production losses. Hence, the knowledge of their operating loads is necessary to determine very exactly. The objective of this article is to identify and verify the basic dynamic parameters of the welding manipulator, as a starting point for the operating loads calculation of linear guiding systems. This issue was solved by combining the measurement of kinematic values and MBS (Multi-body System) analysis in case of the concrete linear welding manipulator, which was the main part of the observed welding line. We have measured time values of acceleration in defined points of the manipulator and evaluated them by FIR (Finite Impulse Response) filter, FFT (Fast Fourier Transformation) analysis and ODS (Operating Deflection Shapes) analysis. The obtained frequency spectrum showed oscillation frequencies, which could be compared with frequencies of the manipulator dynamical model by different mass and stiffness parameters. In this way, the dynamic parameters of the welding manipulator can be identified and used for the next calculations and

---

<sup>1</sup> Faculty of Mechanical Engineering, Technical University of Liberec, Studenstká 2, 460 01 Liberec, Czech Republic. Email: [radka.jirova@tul.cz](mailto:radka.jirova@tul.cz)

<sup>2</sup> Faculty of Mechanical Engineering, Technical University of Liberec, Studenstká 2, 460 01 Liberec, Czech Republic. Email: [lubomir.pesik@tul.cz](mailto:lubomir.pesik@tul.cz)

simulations, where loads of linear guiding systems will produce very important results.

**Keywords:** dynamic parameters, dynamic system, welding production line, welding manipulator, linear guiding system

## 1. INTRODUCTION

Nowadays, during the Industry 4.0, great emphasis is placed on production machines reliability. Operating conditions of all important machines should be thoroughly analysed and evaluated. These precautions should increase their reliability, predict possible failures and prevent possible production losses [4-8,10,11,13-15,17].

In case of welding production lines, a prediction of linear guiding system failures in one of the first places is needed, because these parts enable in these lines the transport of car bodies for the welding process. Should they fail, the production must be stopped for a few days. This situation can lead to significant production losses. Therefore, the prediction of the failures is very necessary and the determination of the linear guiding systems loads is the main task for calculations and simulations on the welding manipulator mechanical model [2,3,16].

To identify these operating loads, it is necessary to have sufficient notions about the dynamical behaviour of the welding manipulator. In this article, the issue is solved as the planar motion of the manipulator.

## 2. MEASUREMENT

In Fig. 1 is displayed the 3D model of the welding manipulator with positions of two acceleration sensors (S-V and S-Z). The major parts of the manipulator are the cart, two so-called Z-axes and two clamping frames with car bodies.

The welding manipulator exercises a translation motion, which is provided by the stepper motor through a rack gear and linear guiding systems. The linear guiding systems connect the cart with the frame by means of guide profiles. However, the elastic construction parts and clearances of linear guiding systems cause oscillations of the manipulator against the meshing point of the rack gear. The rack gear, the stepper motor and linear guiding systems are placed on the cart of the manipulator. The clamping frames with the car bodies are connected to the cart through the Z-axis that enables their vertical translation motion.

Kinematics of the welding manipulator was measured by two three-axis acceleration sensors [12]. The first sensor S-V was situated close to the stepper motor that powers the manipulator. The second one S-Z was situated close to the car bodies clamping frame (Fig. 1). The knowledge of the kinematic parameters in two positions gives sufficient notions about the dynamic system behaviour of the welding manipulator [1].

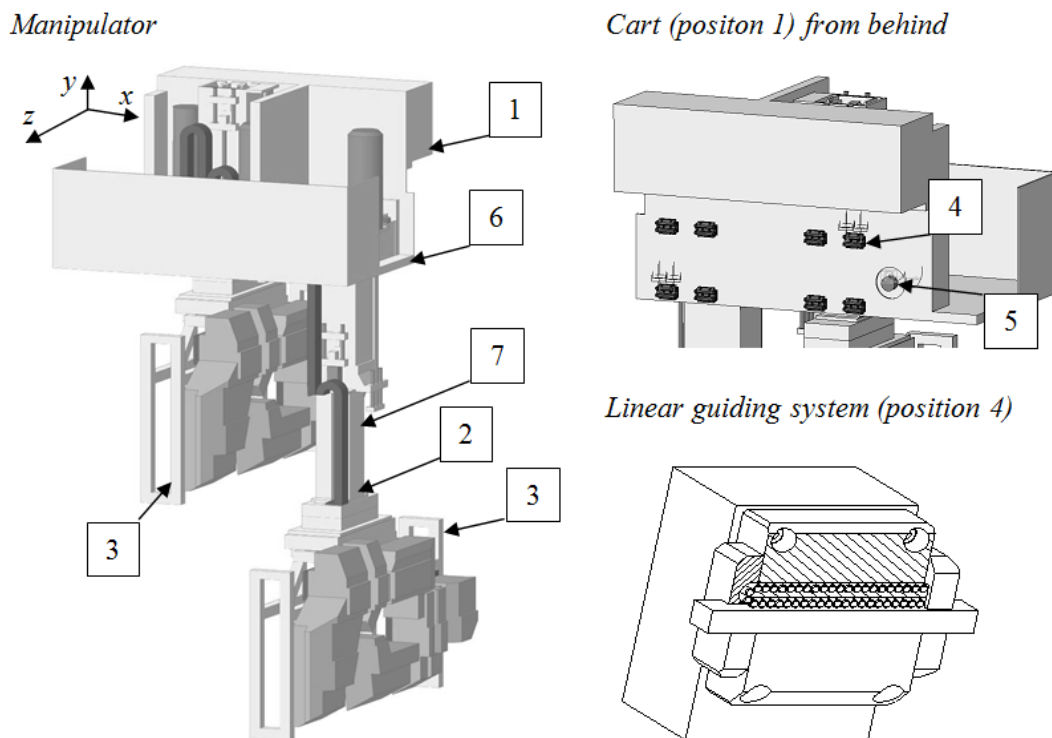


Fig. 1. Model of the welding manipulator with positions of two acceleration sensors:  
 1 - cart, 2 - Z-axis, 3 - clamping frame, 4 - linear guiding system,  
 5 - rack gear, 6 - acceleration sensor S-V, 7 - acceleration sensor S-Z

### 2.1. Finite Impulse Response (FIR) filter

Measured data were evaluated by the FIR filter that enabled the identification of the system basic motion in each coordinate axis. Considering the Fast Fourier Transformation (FFT) analysis result, the FIR filter was used as a low pass filter with the cut-off frequency 3 Hz. The higher order of the filter was used for reaching the sufficient slope of the transition band.

Measured and filtered values are shown in Fig. 2 – Fig. 7. Wherein Fig. 2 shows acceleration measured by the first sensor S-V in the translational direction and its result by FIR filtration. The maximum value of the filtered acceleration was  $1,63 \text{ m/s}^2$ .

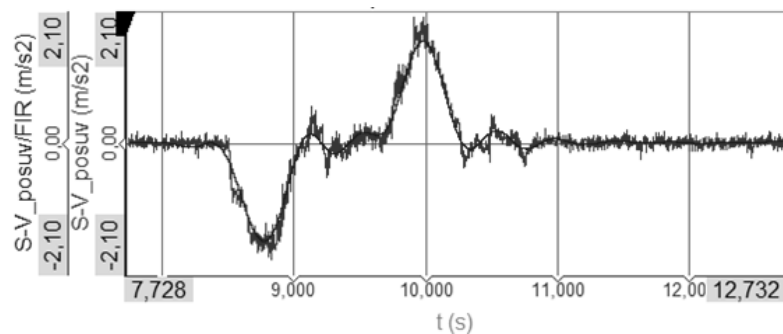


Fig. 2. Acceleration on the place of the sensor S-V in the translational direction – FIR filter

Fig. 3 shows the acceleration measured by the sensor S-V in the vertical direction and its result by FIR filtration. The maximum value of the filtered acceleration was  $0,07 \text{ m/s}^2$ .

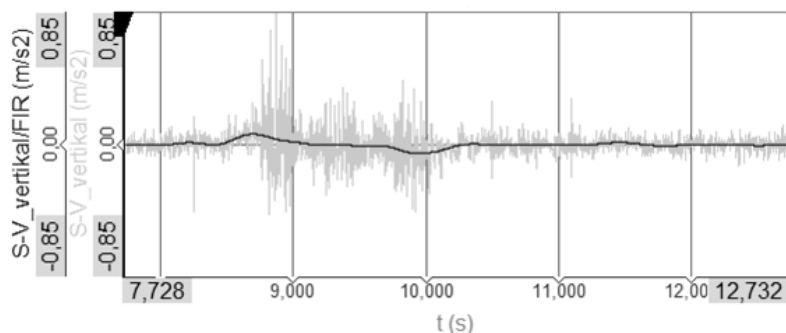


Fig. 3. Acceleration on the place of the sensor S-V in vertical direction – FIR filter

Fig. 4 shows the acceleration measured by the first sensor S-V in the transversal direction and its result by FIR filtration. The maximum value of the filtered acceleration is  $0,18 \text{ m/s}^2$ .

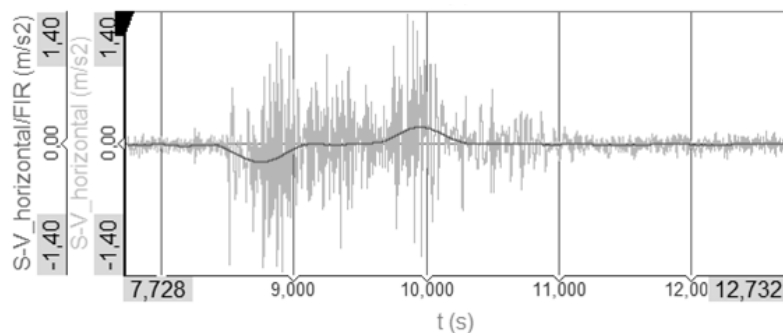


Fig. 4. Acceleration on the place of the sensor S-V in transversal direction – FIR filter

Fig. 5 shows the acceleration measured by the second sensor S-Z in the translational direction and its result by FIR filtration. The maximum value of the filtered acceleration is  $1,74 \text{ m/s}^2$ .

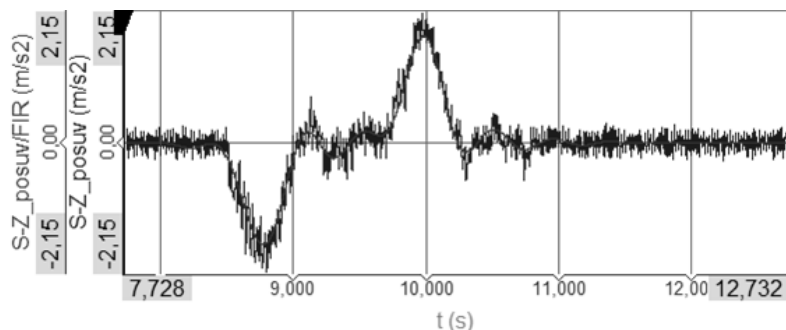


Fig. 5. Acceleration on the place of the sensor S-Z in translational direction – FIR filter

Fig. 6 shows the acceleration measured by the second sensor S-Z in the vertical direction and its result by FIR filtration. The maximum value of the filtered acceleration is  $0,21 \text{ m/s}^2$ .

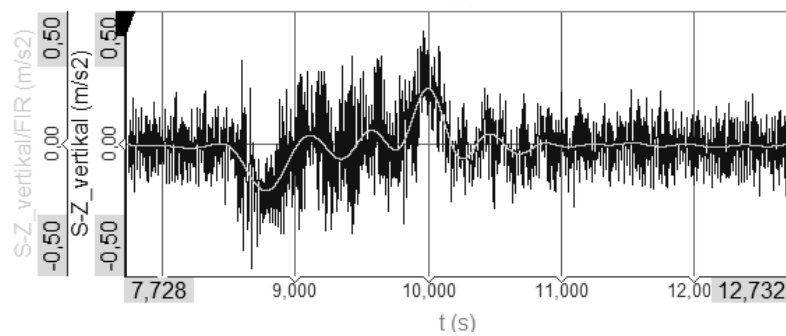


Fig. 6. Acceleration on the place of the sensor S-Z in vertical direction – FIR filter

Fig. 7 shows the acceleration measured by the second sensor S-Z in the transversal direction and its result by FIR filtration. The maximum value of the filtered acceleration is  $0,04 \text{ m/s}^2$ .

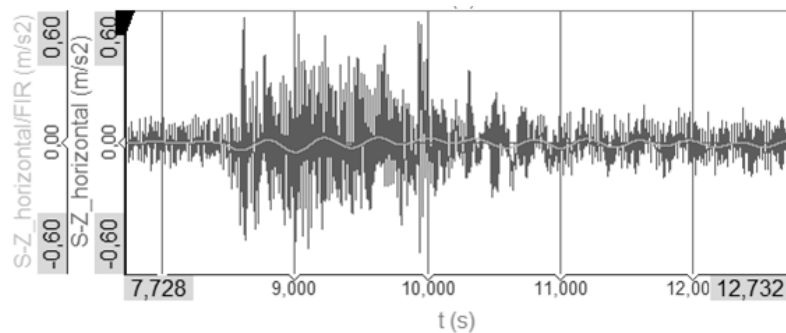


Fig. 7. Acceleration on the place of the sensor S-Z in transversal direction – FIR filter

## 2.2. FFT analysis

The results of the FFT analysis are shown in Fig. 8.

Fig. 8 shows the results of the FFT analysis by previously introduced filtered signals. The basic oscillation frequency of the manipulator is around 1,2 Hz.

## 2.3. Operating Deflection Shapes (ODS) analysis

The ODS analysis was made for the operating frequency 1,2 Hz of the manipulator. Eight one-axis acceleration sensors were placed in the translational direction on the longer Z-axis and on the clamping frame. The result of this analysis is shown in Fig. 9.

## 3. MULTI-BODY SYSTEM (MBS) ANALYSIS

The basis for creating the dynamic model of the manipulator is its 3D model that provides its mass parameters. Kinematic, elastic and damping connections are assigned to the 3D model. The dynamic system of the manipulator has the kinematic excitation, where the acceleration values are given by the data of the stepper motor. The dynamic model with corresponding connections is shown in Fig. 10.

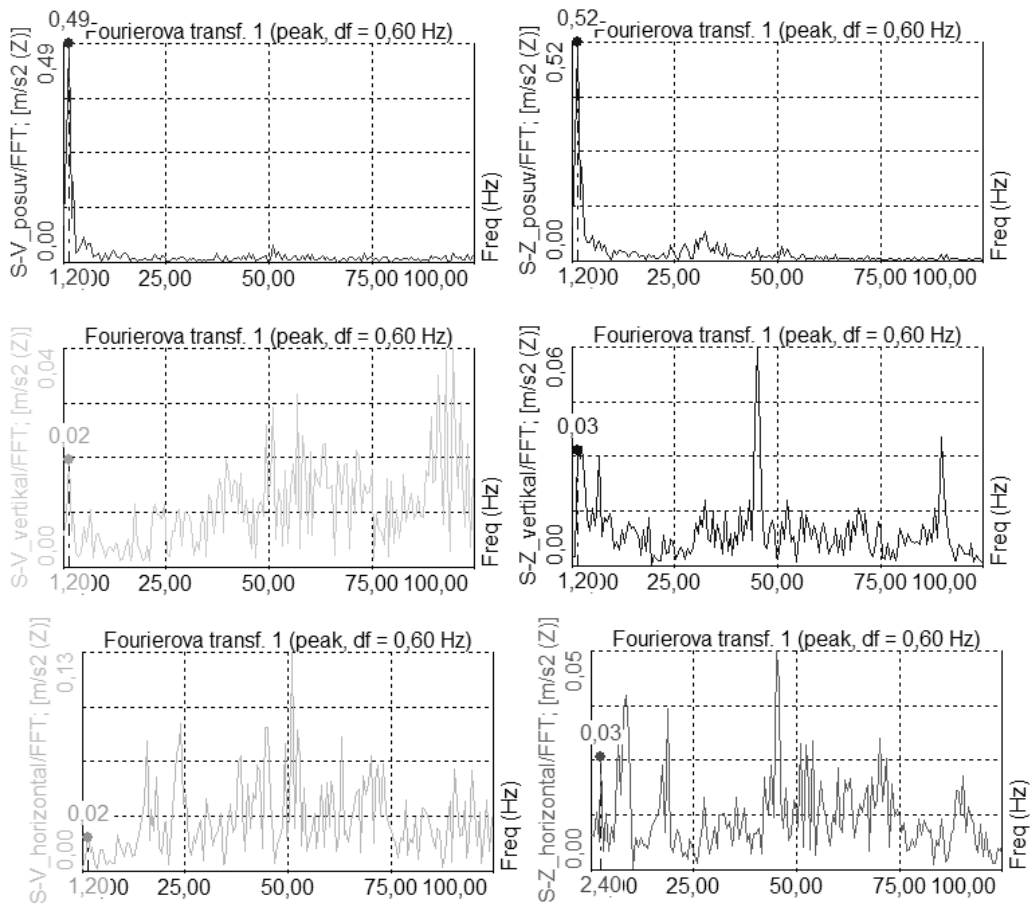


Fig. 8. Frequency spectrum

### 3.1. Elastic and damping parameters of the system

The vertical stiffness of the elastic connection may be calculated:

$$k = \frac{k_{\varphi}}{\sum_{j=1}^n l_n^2} = \frac{J_z (2\pi f)^2}{\sum_{j=1}^n l_n^2}, \quad (1)$$

wherein  $k_{\varphi}$  is the torsion stiffness,  $J_z$  moment of inertia about the  $z$  axis,  $f$  basic oscillation frequency (1,2 Hz) of the manipulator about the  $z$  axis (Fig. 10),  $l$  distance between elastic and damping connections and the rotational point  $L$  and  $n$  number of elastic and damping connections [4].

The vertical damping coefficient is:

$$b = \frac{2\sqrt{J_z k_{\varphi}}}{\sum_{j=1}^n l_n^2} b_{rel}, \quad (2)$$

wherein  $b_{rel}$  is relative damping coefficient.

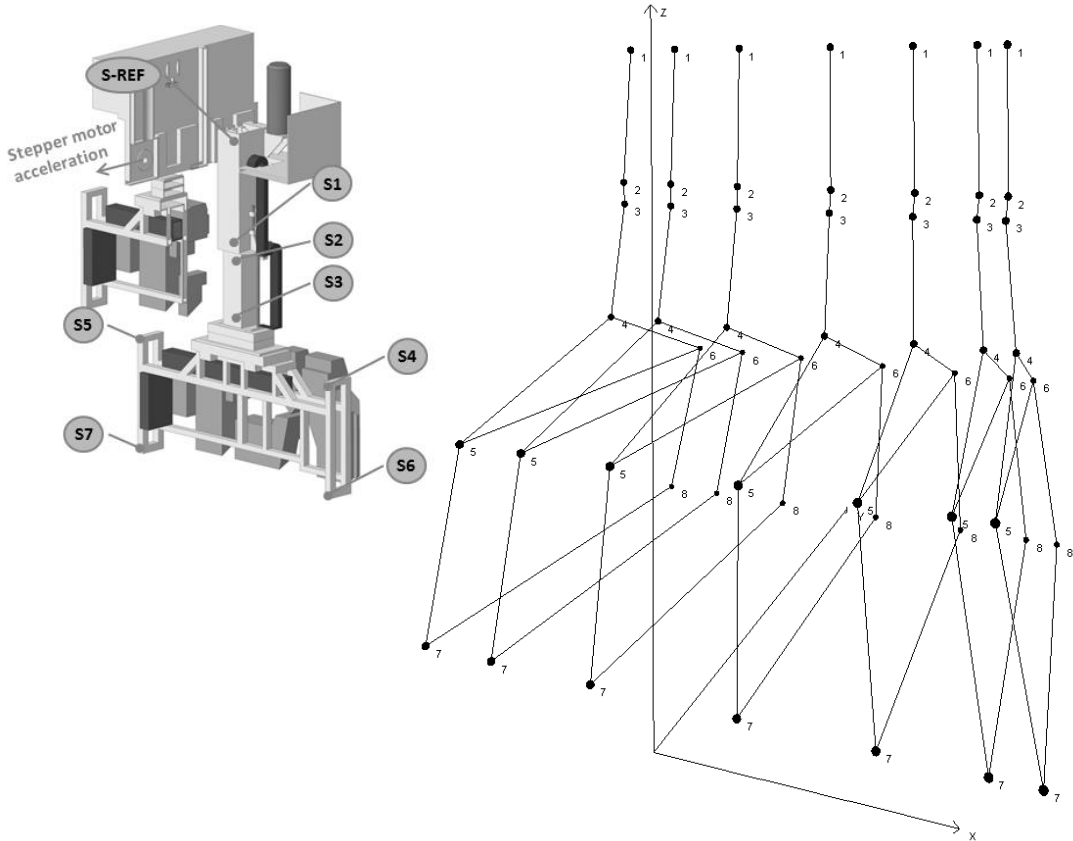


Fig. 9. Operating deflection shapes of the manipulator

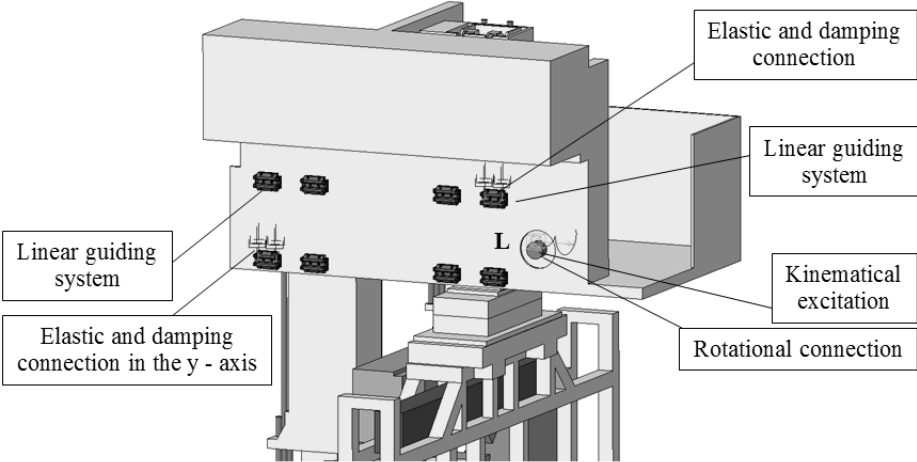


Fig. 10. Connections in the dynamic model of the manipulator

### 3.2. Kinematical excitation

For the kinematical excitation, the time function of the stepper motor velocity and its derivation may be used. This was reached by “the five point method” with equation:

$$a_1(t) = \frac{a_1(t-2)+a_1(t-1)+a_0(t)+a_0(t+1)+a_0(t+2)}{5}, \quad (3)$$

wherein  $a_1$  is new value of acceleration (velocity) and  $a_0$  is last value of acceleration (or velocity).

The final acceleration function used for the kinematical excitation of the system is shown in Fig. 11.

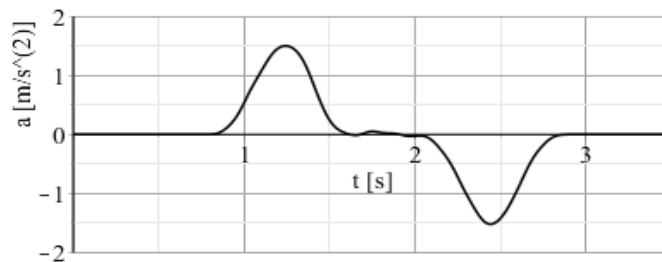


Fig. 11. Kinematical excitation of the manipulator dynamic system

The maximum value analysed of the stepper motor acceleration was  $1,5 \text{ m/s}^2$ .

## 4. COMPARISON OF MEASURED AND SIMULATED ACCELERATION VALUES

Results show the relatively sufficient matching between measured and simulated acceleration values. However, it should be noted that for the achievement of better results, it would be appropriate to solve the system as nonlinear. But in this case, it is necessary to know more input parameters.

The comparison of measured and calculated acceleration values is shown in the following figures. In Fig. 12 is shown the comparison between filtered acceleration values of the first sensor S-V in the translational direction and the acceleration as the simulated result of the MBS analysis in the same direction.

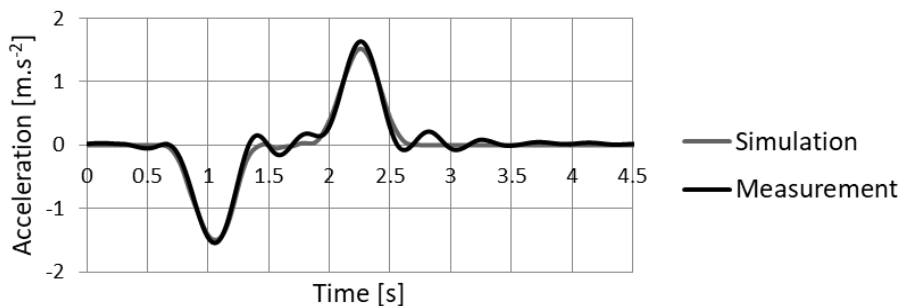


Fig. 12. Acceleration in the place of the sensor S-V in translational direction

Fig. 13 shows comparison between filtered acceleration values of the first sensor S-V in the vertical direction and the acceleration as the simulated result of the MBS analysis in the same direction.

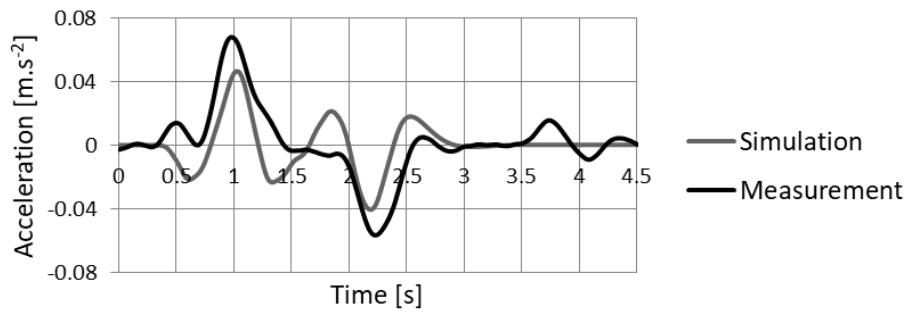


Fig. 13. Acceleration in the place of the sensor S-V in vertical direction

Fig. 14 shows comparison between filtered acceleration values of the second sensor S-V in the translational direction and the acceleration as the simulated result of the MBS analysis in the same direction.

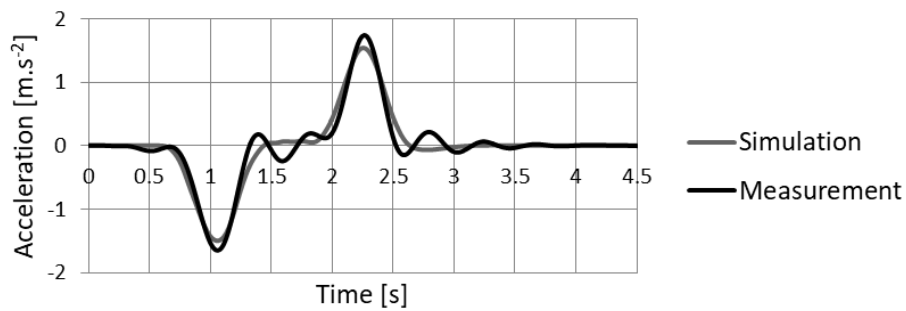


Fig. 14. Acceleration in the place of the sensor S-Z in translational direction

Fig. 15 shows comparison between filtered acceleration values of the second sensor S-V in the vertical direction and the acceleration as the simulated result of the MBS analysis in the same direction.

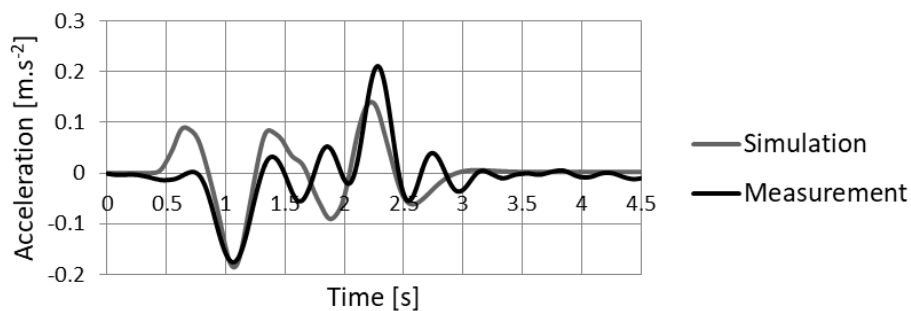


Fig. 15. Acceleration in the place of the sensor S-Z in vertical direction

## 5. CONCLUSIONS

Nowadays, linear guiding systems are used in a wide range of applications, especially for enabling the linear motion of manipulators, robots, transporting parts etc. Usually, the linear guiding systems are present in the very important part of these machines. However, their operating load by the relative complicated dynamic behaviour is not well known, hence, the linear guiding systems might be overloaded, which can lead to their premature failure. Therefore, the knowledge of their operating load is strictly demanded. For the operating load calculation, it is first necessary to identify and verify the dynamical parameters of these machines with the help of the corresponding dynamic model to determine the values of the operating load.

This article illustrates the process of identifying dynamical parameters and their verifications. This process is based on the combination of the measurement and mathematical methods, which can be described in a few steps. First, the process uses measured acceleration values in two points of the moving part. They are evaluated by FIR and FFT. The evaluation of operating deflection shapes can be added for the visualisation of the part oscillation. In the second step, it is necessary to identify mass parameters and elastic and damping parameters of parts connection in the system. 3D modelling and its integrated functions can be used. The system movement can be calculated using the MBS analysis. Finally, the measured kinematical values are compared with the calculated ones. The dynamic parameters are correctly determined in the case of good accordance between the measured and simulated results.

## Acknowledgements

This publication was written at the Technical University of Liberec as part of the project "Vibration damage identification of linear guiding system" with the support of the Specific University Research Grant provided by the Ministry of Education, Youth and Sports of the Czech Republic in 2019.

## References

1. Dresig H., Holzweißig F. 2008. *Maschinendynamik*. [In German: *Machine dynamics*]. Berlin: Springer-Verlag. ISBN 978-3-540-87693-9.
2. Gaska Damian, Tomasz Haniszewski. 2016. "Modelling studies on the use of aluminium alloys in lightweight load-carrying crane structures". *Transport Problems* 11(3): 13-20. DOI: 10.20858/tp.2016.11.3.2. ISSN: 1896-0596.
3. Haniszewski Tomasz, Damian Gaska. 2017. "Numerical modelling of I-Beam jib crane with local stresses in wheel supporting flanges - influence of hoisting speed". *Nase More* 64(1): 7-13. DOI: 10.17818/NM/2017/1.2. ISSN: 0469-6255.
4. Homišin J., R. Grega, P. Kaššay, G. Fedorko, V. Molnár. 2019. „Removal of systematic failure of belt conveyor drive by reducing vibrations”. *Engineering Failure Analysis* 99: 192-202. ISSN 1350-6307.
5. Jacyna Marianna, Mariusz Izdebski, Emilian Szczepański, Paweł Gołda. 2018. „The task assignment of vehicles for a production company”. *Symmetry-Basel* 10(11). Article number: 551.

6. Jacyna-Golda Ilona, Mariusz Izdebski, Emilian Szczepanski. 2016. „Assessment of the method effectiveness for choosing the location of warehouses in the supply network”. *Challenge of Transport Telematics, TST 2016. Communications in Computer and Information Science* 640: 84-97.
7. Jacyna-Golda Ilona, Mariusz Wasiak, Mariusz Izdebski, Konrad Lewczuk, Roland Jachimowski, Dariusz Pyza. 2016. „The evaluation of the efficiency of supply chain configuration”. *Proceedings of the 20th International Scientific Conference Transport Means 2016. Transport Means - Proceedings of the International Conference*: 953-957.
8. Liptai Pavol, Marek Moravec, Ervin Lumnitzer, Marcela Gergel'ová. 2017. „Proposal of the sound insulating measures for a vibrational sorter and verification of the measured effectiveness”. *Advances in Science and Technology-Research Journal* 11(3): 196-203. ISSN 2299-8624. DOI: 10.12913/22998624/76068.
9. Maláková Silvia. 2017. „Analysis of gear wheel body influence on gearing stiffness”. *Acta Mechanica Slovaca* 21(3): 34-39. ISSN 1335-2393.
10. Mazurkiewicz D. 2014. „Computer-aided maintenance and reliability management systems for conveyor belts”. *Eksploatacja i Niezawodność – Maintenance and Reliability* 16(3): 377–382.
11. Mazurkiewicz D. 2010. „Tests of extendability and strength of adhesive-sealed joints in the context of developing a computer system for monitoring the condition of belt joints during conveyor operation”. *Eksploatacja i Niezawodność – Maintenance and Reliability* 3: 34-39.
12. Navrátil M. 1981. *Měření mechanického kmitání. Úvod do teorie snímačů*. [In Czech: *Measurement of mechanical vibration. Introduction to sensor theory*]. Praha: SNTL.
13. Puškár Michal, Melichar Kopas. 2018. „System based on thermal control of the HCCI technology developed for reduction of the vehicle NOX emissions in order to fulfil the future standard Euro 7”. *Science of the Total Environment* 643: 674-680. ISSN 0048-9697. DOI: 10.1016/j.scitotenv.2018.06.082.
14. Sága Milan, Peter Kopas, Milan Uhrčík. 2012. „Modeling and experimental analysis of the aluminium alloy fatigue damage in the case of bending - torsion loading”. *Procedia Engineering*. 48: 599-606. ISSN 1877-7058.
15. Sága Milan, Milan Vaško, Nadežda Čuboňová, Wiesława Piekarska. 2016. *Optimisation algorithms in mechanical engineering applications*. Harlow: Pearson. ISBN 978-1-78449-135-2.
16. Tomeh E. 2015. *Technická diagnostika. Vibrační diagnostika strojů a zařízení*. [In Czech: *Technical diagnostics. Vibration diagnostics of machines and equipment*]. Liberec: Technical university in Liberec. ISBN 978-80-7494-174-0.
17. Zul'ová L., Grega R., Krajňák J. 2017. „Optimization of noisiness of mechanical system by using a pneumatic tuner during a failure of piston machine”. *Engineering Failure Analysis* 79: 845-851. ISSN 1350-6307.

Received 18.11.2019; accepted in revised form 12.01.2020



Scientific Journal of Silesian University of Technology. Series Transport is licensed under a Creative Commons Attribution 4.0 International License